

Document downloaded from:

<http://hdl.handle.net/10251/157500>

This paper must be cited as:

Valero Chuliá, FJ.; Rubio Montoya, FJ.; Besa González, AJ.; Llopis Albert, C. (2019). Efficient trajectory of a car-like mobile robot. *Industrial Robot An International Journal*. 46(2):211-222. <https://doi.org/10.1108/IR-10-2018-0214>



The final publication is available at

<https://doi.org/10.1108/IR-10-2018-0214>

Copyright Emerald

Additional Information

This article is (c) Emerald Group Publishing and permission has been granted for this version to appear here <https://riunet.upv.es/>. Emerald does not grant permission for this article to be further copied/distributed or hosted elsewhere without the express permission from Emerald Group Publishing Limited.

EFFICIENT TRAYECTORY OF AN AUTO-GUIDED MOBILE ROBOT

Francisco Valero, Francisco Rubio, Antonio José Besa, Carlos Llopis-Albert

Universitat Politècnica de València, Valencia

ABSTRACT

Designing efficient manufacturing systems is essential to increase business performance. In this context, the use of Autonomous Guided Vehicles (AGVs) in logistic processes and Material Handling Systems (MHS) improves productivity and reduce costs. However, scheduling operation tasks and routing schemes of AGVs when devising Flexible Manufacturing Systems (FMS) becomes a complex problem. This paper presents an optimization algorithm used to guide AGVs in indoor manufacturing environments that goes a step further regarding the already existing techniques by overcoming certain of their limitations. Its novelty lies in obtaining efficient trajectory without collisions while considering the dynamic constraints of the robot, including the characteristics of power delivery of the motor, the behavior of the tires and basic inertial parameters, which are usually disregarded resulting in very conservative or inaccurate solutions. Furthermore, it provides free ranging routes with lower time and allows considering the effects of different transport weights (products), and AGVs speeds, accelerations, changes in directions and stoppages. The robust, efficient and stable optimization algorithm is based on a recursive procedure that generates minimum-time polynomial trajectories with passing configurations and dynamic constraints and makes use of the Quadratic Programming Algorithm with Distributed and Non-Monotone Line Search (NLPQLP). An experimental validation of the simulation results has been successful carried out in several case studies using a RBK robot, i.e., a real electric vehicle.

Keywords: car-like robot navigation, robot dynamics, obstacle avoidance, optimization, Material Handling Systems (MHS), Flexible Manufacturing Systems (FMS)

1. INTRODUCTION

AGVs are programmable and self-driven vehicles used to transfer loads from one location on the facility to another depending on the task given and within a time window. They can be considered as multiple systems that can operate independently as well as in cooperation with each other. AGVs have gained an increasing focus of attention in recent years in many manufacturing applications. They play a major role in the Material Handling Systems (MHS) within indoor facilities and have many applications in manufacturing and logistics processes. They also lead to achieving Flexible Manufacturing Systems (FMS) (Llopis-Albert et al., 2018). Then the AGV network flow can be easily redesigned to accommodate frequent changes, for instance, in manufacturing different products or changes in demand. The deployment of automated technologies in manufacturing facilities have led to great benefits, which comprise an increase of the system efficiency, a reduction of operational cost and an increase of the work precision. Additionally, they considerably reduce the number of work accidents related to transports and warehouse activities if compared with human operators. Note that occupational

health and safety is a major concern nowadays. Moreover, AGVs carries out the manufacturing tasks at low cost if compared to other conveyor systems for moving material through the facility such as conveyors, chains, etc.

With regard to the technical characteristics of these mobile robots they should be able to move autonomously and have an efficient navigation system that allows it to carry out its task during transit from an initial to a final configuration.

Part of the function assigned to a robot's navigation system consists of planning the trajectory, which considers three fundamental aspects: a) the locomotion system, b) its dynamic behavior, which includes the consideration of the driving forces, resistance forces and the inertial characteristics of the robot and c) the environment in which it will move and its representation, considering the possible existence of obstacles. Normally, in the process of obtaining the trajectory, it is worth minimizing certain working variables such as the time or energy consumed.

In autonomous car-like robots, the behavior of the locomotion system is highly conditioned by the wheels and their interaction with the terrain. It is necessary to take into account their capacities in the transmission of the actions of the engine and brakes to the ground, since they are key determinants of the car-like robot's dynamic response. As for the modeling of the environment and the representation of the space through which the robot will move, it is a topic that has been investigated for decades with efficient techniques for the detection of collisions.

A brief summary of the techniques used for modeling the environment and for the representation of space from the 1980s to the present day includes the generalized cones method [1], graph search techniques, roadmaps, Voronoi diagrams [2], and visibility graphs. A recent example of visibility graphs can be found in [3]. In [4] the authors introduce a bug algorithm that solves the problem of navigation without using any map or model of the environment, using only the data from the sensors.

The Quadtree representation technique and decomposition in cells ([5] and [6]) must also be cited. A summary of the techniques for modeling the environment applied to path planning can be found in [7], where some of the strengths and weaknesses of the presented methods are discussed. An application of some of the algorithms (techniques based on searches in graphs like the A* algorithm, the greedy search or the uniform cost search) are shown in [8]. And a summary of the state of the art and future lines of research in relation to motion planning for autonomous robots can be found in [9]. In [10] the main objective of the algorithm is to find, if it exists, an efficient path between cells in a given binary map, using the grid occupation matrix, as discussed in González-Arjona et al. [11].

As for the dynamic behavior of the vehicle, several trends can be observed in the literature. One is to consider or reduce the car-like robot to a point as in [12], where the authors analyze the planning of trajectories, imposing restrictions on energy during its motion. This limits the speed and acceleration values given by the actuators, namely an electric DC brush motor. In fact, the dynamic characteristics of the car-like robot, such as masses and inertias, are not taken into account, nor are considerations of the contact forces between tire and ground. Neither do they include any considerations about changes in the direction of motion. However, these are aspects that are essential for good trajectory planning.

Another tendency is to use the full car model of the car-like robot as in [13], where the authors present a kinematic model of the vehicle; however, the kinematic considerations are limited to imposing restrictions on speeds and accelerations without considering dynamic restrictions associated with masses and inertia of the vehicle or the behavior of the tire. In this work the paths are obtained by introducing kinematic constraints to follow curves of the cubic polynomial type, trigonometric splines and clothoids.

In [14] and [15] the vehicle is also modeled as a full car. In [14], the same authors state that they do not use a dynamic model since at low speeds the kinematic model is sufficient to obtain computationally feasible results. When velocities are important or masses are not negligible, the dynamic model must be introduced.

A novel integrated local trajectory planning and tracking control (ILTPTC) framework for autonomous vehicles driving along a reference path with obstacle avoidance is presented in [15]. However, they do not consider the interactions between the ground and the tire and, in fact, the trajectory planning is limited to the generation of an optimum path with a specific profile of speeds without dynamic considerations. They limit the velocity of the vehicle, taking into account considerations such as the state of the road and traffic rules. And they limit the lateral acceleration so as not to have to take into account the effects of drift and rolling on the stability of the vehicle. They also limit linear acceleration in order to limit maximum velocity.

Another trajectory planner is presented for a full car-like mobile robot in [16], where the kinematic principles are accurately described by differential equations and the constraints are strictly expressed using algebraic inequalities. Although it tries to describe the trajectory in terms of the corresponding differential equations, it does not take into account the driving forces, interaction with the terrain or inertial characteristics of the system.

In the cited works, the trajectory of the vehicle is determined on the basis of kinematic considerations, limiting the velocity values due to the characteristics of the actuators, especially those of the electric motors, or other issues. They do not really take into account the inertial characteristics of the mobile robot or use any model of tire.

A third trend in trajectory planning is represented by authors who work with the simplified dynamic model of the robot, considering a system with few degrees of freedom. In [17] the authors use the bicycle model of a four-wheel-steering (4WS) vehicle. The limits of vehicle mechanism, drive and brake torque are taken into account and dynamic constraints are replaced by velocity kinematics and acceleration based on inertial and friction parameters. However, it does not include lateral tire friction limits.

In this paper, the authors present a planner for obtaining trajectories for mobile robots with wheels, which considers the basic dynamic properties of the robot, including the lateral friction limit of the tires, motor and brake torques, obtaining feasible and efficient trajectories for the robot based on the recursive resolution of optimization problems.

It is a global planner that makes it possible to obtain trajectories considering the constraints associated with the dynamics of the robot in an environment with stationary obstacles. The procedure is based on the determination of passing configurations between which the path is

adjusted by polynomial interpolation functions whose coefficients are determined to minimize the time while respecting the dynamic constraints of the vehicle, thus defining the trajectory.

To minimize the time, a Quadratic Programming Algorithm with Distributed and Non-Monotone Line Search (NLPQLP) is used, which was proposed and developed by Schittkowski ([18] and [19]).

This approach marks a clear difference from planners that only include kinematic constraints, as in Simba et al. [20] and [21], or that are conservative or do not guarantee the feasibility of trajectories, as in Li et al. [22] and Tokekar et al. [23]. Also it is different from [24] in which the authors analyse the minimum-energy translational trajectory generation for a two-wheeled mobile robot. The authors simplify too much the model so that they only consider a WMR moving in a straight line. Also the dynamics of the whole vehicle are neglected.

This article presents a novel methodology to deal with the trajectory generator for a car-like robot, which introduces several advantages regarding previous approaches. It is organized as follows: Section 2 introduces the concepts and definitions used in modeling the trajectory. Section 3 presents the procedure for obtaining the efficient trajectory without collisions. Section 4 details the kinematic and dynamic restrictions used in optimization problems, as well as the modeling of the car-like robot from which the constraints are obtained. The simulation results and an experimental validation is presented in Section 5 through three examples of application. In the last section, the conclusions are summarized.

2. MODELING THE TRAJECTORY

This section details the definitions and procedures used to obtain the trajectory of the car-like robot in the plane.

2.1. Definitions.

2.1.1. Local reference system. It is sited on the center of gravity of the robot and an ISO reference system is associated with it.

2.1.2. Position. The position of the robot is defined by the location of the origin of the local reference system, $p(x, y)$.

2.1.3. Configuration. The configuration of the robot is defined by the position and orientation of the local reference system, $c(p, \theta)$. A configuration is said to be feasible when it belongs to a trajectory and has no collision.

2.1.4. Adjacent position. Given a feasible configuration of the robot c_j , it is said that p_k is adjacent to it if it has been obtained by increasing the coordinates corresponding to the position of c_j .

2.1.5. Obstacle. It is static and is defined by a combination of pattern obstacles, circles and polygons that determine forbidden zones for the robot.

2.1.6. Interval. Given two positions of the robot p_j and p_k , the interval I_j will be defined by the polynomials of the form:

$$\begin{aligned} \forall t \in [0, t_j]; \\ x_j &= a_{xj} + b_{xj}t + d_{xj}t^2 + e_{xj}t^3 \\ y_j &= a_{yj} + b_{yj}t + d_{yj}t^2 + e_{yj}t^3 \end{aligned} \quad (1)$$

where t is the variable time associated with the motion of the robot, and the following must be fulfilled:

$$\left. \begin{array}{l} x_j(0) = x_j \\ y_j(0) = y_j \end{array} \right\} \text{and} \left. \begin{array}{l} x_j(t_j) = x_k \\ y_j(t_j) = y_k \end{array} \right\}$$

2.1.7. Trajectory. Given a sequence of m robot positions, $P = \{p_1, p_2, \dots, p_m\}$, a trajectory T is defined by a sequence of $m-1$ intervals between the positions of P that satisfies:

- Continuity in positions.

$$\left. \begin{array}{l} x_j(0) = x_j \\ y_j(0) = y_j \end{array} \right\} \text{and} \left. \begin{array}{l} x_j(t_j) = x_{j+1} \\ y_j(t_j) = y_{j+1} \end{array} \right\}$$

(4 $(m-1)$) equations are set.

- Continuity in velocities.

The initial and final velocities of the trajectory must be zero,

$$\left. \begin{array}{l} \dot{x}_1(0) = 0 \\ \dot{y}_1(0) = 0 \end{array} \right\} \text{and} \left. \begin{array}{l} \dot{x}_{m-1}(t_m) = 0 \\ \dot{y}_{m-1}(t_m) = 0 \end{array} \right\}$$

4 equations are set.

The initial velocity of each interval must be equal to the final velocity of the previous one,

$$\left. \begin{array}{l} \dot{x}_j(0) = \dot{x}_{j-1}(t_{j-1}) \\ \dot{y}_j(0) = \dot{y}_{j-1}(t_{j-1}) \end{array} \right\}$$

(2 $(m-2)$) equations are set.

- Continuity in accelerations.

The initial acceleration of each interval must be equal to the end of the previous one,

$$\left. \begin{array}{l} \ddot{x}_j(0) = \ddot{x}_{j-1}(t_{j-1}) \\ \ddot{y}_j(0) = \ddot{y}_{j-1}(t_{j-1}) \end{array} \right\}$$

(2 $(m-2)$) equations are set.

Once the times associated with the different intervals forming the trajectory are known, a linear system of (8 $(m-1)$) equations is available, which makes it possible to obtain the coefficients of the polynomials (1) that define the intervals so that the trajectory is fully determined.

2.1.8. Minimum time trajectory T^{min} . It is said that a trajectory has the minimum time when the motion of the mobile robot when executing it fulfills all the imposed kinematic and dynamic restrictions, and the sum of the times associated with the intervals is minimum.

2.1.9. Offspring trajectory. It is said that a trajectory T_k^{min} is an offspring from another T_j^{min} with a sequence of m positions when the sequence of positions of T_k^{min} is equal to that of T_j^{min} plus one, provided that the position added is not the first or the last one:

$$P^k = P^j \cup p_n, \text{ for } n \neq 1 \text{ and } n \neq m+1.$$

The offspring trajectories from several generations will have different numbers of intervals but they will always maintain the same initial and final positions.

2.1.10. Trajectory Space. For a robot with a given initial position p_i and a final position p_f , the configuration space TS is defined as the set of minimum time trajectories between p_i and p_f . When the robot operates in an environment with obstacles, the subspace of TS formed by the trajectories without collisions will be represented as TS^c .

2.2. Generation of a minimum time trajectory.

For a known mobile robot, which has explicit equations for the kinematic and dynamic constraints as described below, given the initial configuration c_i , the final position p_f and a series

of $(m-1)$ passing positions p_j with $j=1 \dots m-1$, an optimization problem to obtain the minimum time trajectory T^{min} associated with the sequence of positions $P = \{p_i, \dots, p_j, \dots, p_f\}$ is set.

In the following subsections the characteristics of the proposed optimization problem are detailed.

2.2.1. Objective function. The trajectory will consist of m intervals between the $m + 1$ positions of P , where t_j for $j=1, m$ are the times associated with the intervals that comply with the equations of type (1) and the conditions associated with the definition in section 2.1.7, so that the objective function is:

$$f(t) = \sum_{j=1}^m t_j \quad (2)$$

2.2.2. Constraints:

- i. Initial orientation θ_i , corresponding to the initial configuration c_i .
- ii. The steering wheel angle does not exceed a specified value δ_{max} .
- iii. The maximum speed of the vehicle cannot exceed V_{max} .
- iv. The driving force is limited by the torque curve of the engine.
- v. The adhesion of the tires to the terrain is limited.

This is an optimization problem with nonlinear constraints, whose solution is obtained by the NLPQLP Quadratic Programming Algorithm with Distributed and Non-Monotone Line Search created and proposed by Professor Klaus Schittkowski. It should be considered that, in each iteration, the linear system associated with obtaining the coefficients of the equations of type (1) will be solved using the normalized time method [26] so as not to penalize the computation times and, additionally, the derivatives of the constraints are obtained by finite differences.

3. GENERATION OF THE TRAJECTORY WITHOUT COLLISIONS

The problem is to obtain an efficient and collision-free trajectory for a mobile robot in an environment with static obstacles. An efficient trajectory is understood to be one that is near the minimum time with a low computational cost and which respects the restrictions imposed on the robot in Section 2.2.2. Collision detection is specific for each type of standard obstacle, considering the mobile robot as a rectangular shape that is delimited by four segments. For circles, the distance from each segment to the center of the circle is calculated and if it exceeds the radius there is no collision. For polygons, it is verified that there is no intersection between the segments corresponding to mobile robot and those of the obstacles.

The initial data are:

- Information about the robot that is needed for its modeling, as described in section 4.
- Information about obstacles and their locations.
- Initial configuration and final position of the mobile robot.

The steps followed to generate the trajectory are similar to those employed by Rubio et al., in [25] on a PUMA robot with fixed base, but adapted to the needs of the mobile robot, resulting:

- a. Calculation of the minimum time initial trajectory.
- b. The trajectory T_i^{min} is obtained from a single interval with $P^i = \{p_i, p_f\}$.
- c. Search for collisions.

- d. On the trajectory T_i^{min} , the first configuration with collision c_c is identified, as is the one previous to it c_a . (Figures 1a) and 1b)).
- e. Generation of adjacent positions.
- Four adjacent positions are generated from c_a according to definition 2.1.4, $(p_{aj}, j=1, \dots, 4)$ (Figure 1)) by choosing the positions that are far enough from any obstacle p_{ak} ($0 \leq k \leq 4$); if none exists ($k=0$), a configuration in the previous trajectory c_{a-1} is searched for, and the algorithm works recursively until it finds a configuration that results in ($k \neq 0$).
- f. Generation of offspring trajectories.
- For each of the adjacent positions generated in c. that are not contained within an obstacle, an offspring trajectory T_k^{min} ($0 \leq k \leq 4$) associated with $P^k = P^i \cup p_{a,k}$ is generated. P^i has the initial configuration, the target and the crossing points of the trajectory where the collision has been located (Figure 1)).

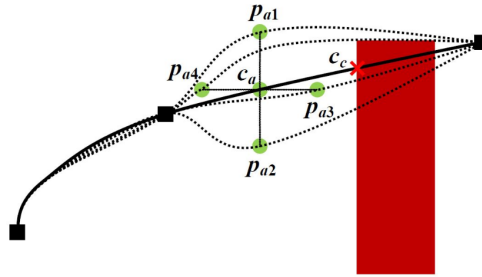


Figure 1. Generation of offspring trajectories.

- g. Selection of the trajectory.
- The trajectories generated in point d. are placed in a set of trajectories ordered by time $TS_t = \{T_1^{min} \dots T_p^{min}\}$. The minimum time trajectory within the set T_1^{min} is selected, taken out of TS_t and also checked for collisions. If there are any collisions, the algorithm returns to point c. This process is repeated (iterating) until a solution T_1^{min} without a collision is reached.

4. MODELING THE CONSTRAINTS

The proposed optimization problem for obtaining the minimum time trajectories T^{min} in section 2.2 requires expressions of reduced complexity that allow iterative calculations to be performed efficiently. The use of dynamic constraints in this type of applications is highly conditioned by computational times, which is why simplified, efficient models are used.

4.1. Robot Modeling.

The RBK robot is an electric vehicle for internal transport powered by a hydrogen fuel cell and batteries with autonomous operation capacity (Figure 2). Its main features are rear-wheel drive, steering on the front wheels, power 3.3 kW, mass 690 kg, top speed 32 km/h, length 2.66 m, width 1.23 m, height 1.70 m, wheelbase $L = 1.65$ m, height of the center of gravity (G) $h = 0.50$ m, distance from G to the front axle $L_a = 1.10$ m, distance from G to the front axle $L_b = 0.55$ m (Figure 3). The model used is based on the well-known "bicycle model", which gives rise to the following simplifying assumptions:

- I. No roll and pitch motions.
- II. No side-load transfer.

- III. No aerodynamic effects.
- IV. A plane model with three degrees of freedom and a restriction associated with the steering angle.
- V. The front wheels are simplified into one that will exert the force corresponding to both, and the same simplification applies to the rear wheels.
- VI. The steering angle corresponds to that of the single front wheel of the model.
- VII. The sideslip and steering angles are small.



Figure 2. Car-Like mobile robot

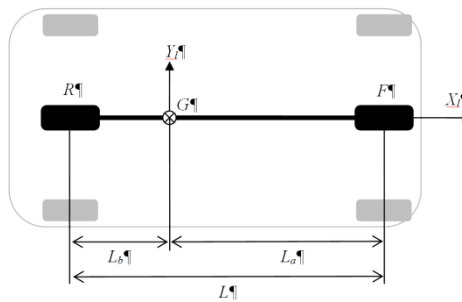


Figure 3. Bicycle model

The kinematics of the center of gravity of the vehicle on the trajectory are known, so in the global reference system, the following expressions are met:

Position of the center of gravity,

$$\begin{aligned} x_G &= a_x + b_x t + d_x t^2 + e_x t^3 \\ y_G &= a_y + b_y t + d_y t^2 + e_y t^3 \end{aligned} \quad (3)$$

Velocity of the center of gravity,

$$\vec{V}_G = \dot{x}_G \vec{i} + \dot{y}_G \vec{j}$$

and its magnitude

$$|\vec{V}_G| = \sqrt{\dot{x}_G^2 + \dot{y}_G^2} \quad (4)$$

Orientation of the velocity of the center of gravity,

$$\theta = \tan^{-1} \frac{\dot{y}_G}{\dot{x}_G} \quad (5)$$

Angular velocity, where β is the sideslip of the mobile robot (Figure 4), which is assumed to be small according to the hypothesis,

$$\omega = \dot{\theta} + \dot{\beta}$$

$\dot{\beta}$ is considered negligible, resulting in,

$$\omega = \frac{\dot{x}_G \ddot{y}_G - \dot{y}_G \ddot{x}_G}{\dot{x}_G^2 + \dot{y}_G^2} \quad (6)$$

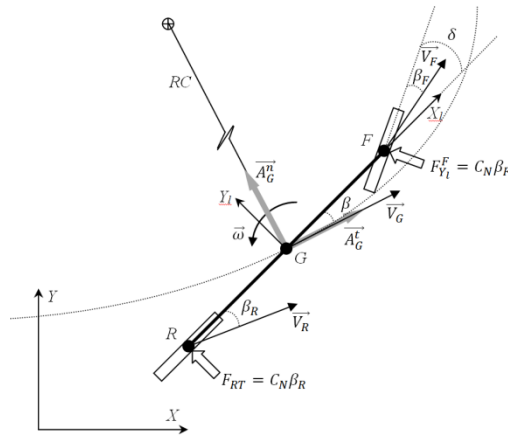


Figure 4. Kinematics and sideslip angles

In a local reference system that is linked to the vehicle according to the ISO convention, the velocity of the rear axle is,

$$\vec{V}_R^l = \vec{V}_G^l + \vec{\omega} \wedge \vec{r}_{GR}$$

so that,

$$\vec{V}_R^l = |\vec{V}_G^l| \cos \beta \vec{i}_l + (|\vec{V}_G^l| \sin \beta - L_b \omega) \vec{j}_l$$

and considering the small sideslip hypothesis,

$$\vec{V}_R^l \approx |\vec{V}_G^l| \vec{i}_l + (|\vec{V}_G^l| \beta - L_b \omega) \vec{j}_l \quad (7)$$

based on the velocity components, the sideslip of the rear axle is obtained,

$$\beta_R = \tan^{-1} \frac{(|\vec{V}_G^l| \beta - L_b \omega)}{|\vec{V}_G^l|}$$

and using the small sideslip hypothesis,

$$\beta_R \approx \beta - \frac{(\dot{x}_G \dot{y}_G - \dot{y}_G \dot{x}_G) L_b}{(\dot{x}_G^2 + \dot{y}_G^2)^{3/2}} \quad (8)$$

with an approach similar to that used to obtain (7), for the front axle,

$$\vec{V}_F^l \approx |\vec{V}_G^l| \vec{i}_l + (|\vec{V}_G^l| \beta + L_a \omega) \vec{j}_l \quad (9)$$

since δ the steering angle is small according to the hypotheses, similar to (8), the forward sideslip is,

$$\beta_F \approx \delta - \beta - \frac{(\dot{x}_G \dot{y}_G - \dot{y}_G \dot{x}_G) L_a}{(\dot{x}_G^2 + \dot{y}_G^2)^{3/2}} \quad (10)$$

The normal acceleration for the trajectory in G is,

$$A_G^n = -\ddot{x}_G \sin \theta + \ddot{y}_G \cos \theta \quad (11)$$

and the tangential acceleration,

$$A_G^t = \ddot{x}_G \cos \theta + \ddot{y}_G \sin \theta \quad (12)$$

In the local reference system that is linked to the vehicle, the lateral acceleration (direction Y_l) is

$$A_G^{Y_l} = A_G^n \cos \beta - A_G^t \sin \beta$$

since the angle β is small, the equation can be written as,

$$A_G^{Y_l} \approx A_G^n - A_G^t \beta \quad (13)$$

Under the small sideslip hypothesis, it is usual to consider the lateral behavior of the tires linearly, so as the front and rear tires are equal, the lateral forces are:

$$F_{RT} = -C_T \beta_R \quad (14)$$

$$F_{FT} = -C_T \beta_F$$

with a direction normal to the rim and opposite to the sideslip (Figure 4).

Setting the Newton-Euler equations for the lateral forces and the moments, the following expression is met,

$$F_{RT} + F_{FT} \cos \delta = m A_G^{Y_l}$$

considering δ small,

$$F_{RT} + F_{FT} = m A_G^{Y_l} \quad (15)$$

The equation of moments is,

$$F_{FT} \cos \delta L_a - F_{RT} L_b = I_z \dot{\omega}$$

where I_z is the moment of inertia of the vehicle around an axis parallel to Z passing through G , taking the usual simplifications and performing the following operation,

$$C_T(-L_a \beta_F + L_b \beta_R) = I_z \dot{\omega} \quad (16)$$

Substituting in equations (15) and (16), β and δ are obtained by solving the linear system.

From equations (8) and (10), β_F and β_R are obtained.

4.2. Constraint associated with the initial orientation.

The mobile robot must start moving from an initial configuration $c_i (p_i, \theta_i)$ and from zero velocity, so the initial acceleration must have the orientation θ_i

$$\tan \theta_i = \frac{d_{y1}}{d_{x1}}$$

d_{x1} and d_{y1} being coefficients of the polynomials (1) corresponding to the first interval of the trajectory, so the corresponding constraint is

$$\tan \theta_i - \frac{d_{y1}}{d_{x1}} = 0 \quad (17)$$

4.3. Constraint of the steering angle.

For each interval i of the trajectory, $\delta(t_{ij})$ is obtained in a discrete number of points j , so that

$$\delta_i = \max(\delta(t_{ij}))$$

and for each interval, the imposed constraint is

$$\delta_{max}^2 - \delta_i^2 > 0, \forall i \quad (18)$$

4.4. Constraint of maximum velocity.

For each interval i of the trajectory, $|\overrightarrow{V}_G(t_{ij})|$ is obtained from equation (4) in a discrete number of points j , so that

$$V_{Gi}^2 = \max(|\overrightarrow{V}_G(t_{ij})|^2)$$

and for each interval, the imposed constraint is,

$$V_{max}^2 - V_{Gi}^2 > 0, \forall i \quad (19)$$

4.5. Constraints associated with forces on tires.

Tire forces due to contact and adherence to the terrain can be written in local coordinates, as:

$$\left. \begin{aligned} \vec{F}_F &= F_F^{x_l} \vec{i}_l + F_F^{y_l} \vec{j}_l + F_F^{z_l} \vec{k}_l \\ \vec{F}_R &= F_R^{x_l} \vec{i}_l + F_R^{y_l} \vec{j}_l + F_R^{z_l} \vec{k}_l \end{aligned} \right\} \quad (20)$$

In X_l direction, assuming a small steering angle, the following equilibrium equation is set:

$$F_F^{x_l} + F_R^{x_l} = mA_{x_l} \quad (21)$$

where A_{x_l} is the acceleration,

$$A_{x_l} = m(\ddot{x}_G \cos(\beta + \theta) + \ddot{y}_G \sin(\beta + \theta))$$

The force on the front wheel is,

$$\left. \begin{aligned} A_{x_l} > 0 &\rightarrow F_F^{x_l} = 0 \\ A_{x_l} \leq 0 &\rightarrow F_F^{x_l} = 0.6 mA_{x_l} + F_{F_r}^{x_l} \end{aligned} \right\} \quad (22)$$

with losses due to rolling motion,

$$F_{F_r}^{x_l} = \mu_r F_F^{z_l} \quad (23)$$

where μ_r is considered constant because the velocity and sideslip angles are small.

The force on the rear wheel is,

$$\left. \begin{aligned} A_{x_l} > 0 &\rightarrow F_R^{x_l} = mA_{x_l} + F_{R_r}^{x_l} + F_{F_r}^{x_l} \\ A_{x_l} \leq 0 &\rightarrow F_R^{x_l} = 0.4 mA_{x_l} + F_{R_r}^{x_l} \end{aligned} \right\} \quad (24)$$

with,

$$F_{R_r}^{x_l} = \mu_r F_R^{z_l} \quad (25)$$

In Y_l direction, considering small steering and sideslips angles, the forces are:

$$\left. \begin{aligned} F_F^{y_l} &= -C_n \beta_F \\ F_R^{y_l} &= -C_n \beta_R \end{aligned} \right\} \quad (26)$$

where C_n is a characteristic of the tire.

In Z_l direction, considering the load transfer due to the acceleration A_{x_l} , the force is:

$$\left. \begin{aligned} F_F^{z_l} &= \frac{m}{L} (L_b g - A_{x_l} h) \\ F_R^{z_l} &= \frac{m}{L} (L_a g - A_{x_l} h) \end{aligned} \right\} \quad (27)$$

Considering a friction circle to limit the maximum force that can be transmitted between the tires and the ground due to the coefficient of friction μ_t , the following condition is obtained:

$$\left. \begin{aligned} \sqrt{(F_F^{x_l})^2 + (F_F^{y_l})^2} &< \mu_t F_F^{z_l} \\ \sqrt{(F_R^{x_l})^2 + (F_R^{y_l})^2} &< \mu_t F_R^{z_l} \end{aligned} \right\} \quad (28)$$

Each interval i of the trajectory is discretized into a discrete number of points, obtaining for each point j the force $F_{F,Rij}^{z_l}$ from equation (27), $F_{F,Rij}^{x_l}$ considering equations (22) to (25) and $F_{F,Rij}^{y_l}$ from equation (26). For each interval and each wheel, the boundary condition established in (28) is considered,

$$\begin{aligned} RT_{F_i} &= \min \left[\left(\mu_t F_{F_{ij}}^{z_l} \right)^2 - \left(F_{F_{ij}}^{x_l^2} + F_{F_{ij}}^{y_l^2} \right) \right] \\ RT_{R_i} &= \min \left[\left(\mu_t F_{R_{ij}}^{z_l} \right)^2 - \left(F_{R_{ij}}^{x_l^2} + F_{R_{ij}}^{y_l^2} \right) \right] \end{aligned}$$

The following two constraints are obtained for each interval of the trajectory:

$$\left. \begin{aligned} RT_{F_i} &> 0 \\ RT_{R_i} &> 0 \end{aligned} \right\} \forall i \quad (29)$$

4.6. Constraint of the driving force.

The traction of the vehicle is achieved by means of an electric motor and a gear reduction of velocity on the rear wheels. The maximum torque transmitted to the driving wheel as a function of its rotation velocity is shown in Figure 5, obtaining from this curve the maximum available driving force $F_{Rmax}^{x_l}$ as a function of the wheel velocity $V_R^{x_l}$ associated with equation (30).

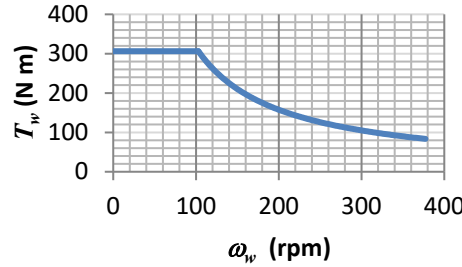


Figure 5. Maximum Driving torque in relation to rotation velocity of the wheel

This behavior is adjusted by the following expressions:

$$\left. \begin{aligned} 0 < V_R^{x_l} \leq 2,42 \frac{m}{s} &\rightarrow F_{Rmax}^{x_l} = 1361 N \\ 2,42 < V_R^{x_l} \leq 8,89 \frac{m}{s} &\rightarrow F_{Rmax}^{x_l} = \frac{3300}{V_R^{x_l}} N \end{aligned} \right\} \quad (30)$$

For each interval i of the trajectory, $F_R^{x_l}(t_{ij})$ and $F_{Rmax}^{x_l}(t_{ij})$ are obtained in a discrete number of points j , and considering

$$RF_i = \min \left(F_{Rmax}^{x_l}(t_{ij}) - F_R^{x_l}(t_{ij}) \right), \text{ the constraints being:} \\ RF_i > 0, \forall i \quad (31)$$

5. SIMULATION AND EXPERIMENTAL RESULTS

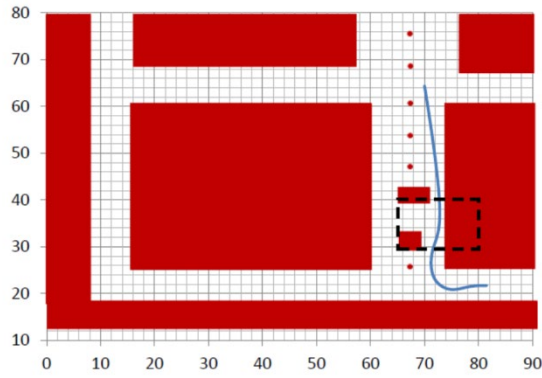
Four examples are presented to illustrate the behavior and the quality of the algorithm. In the first two, the same initial configuration is used to reach different points, and in the third one, very distant points within the chosen space are used to work with. In addition, an experimental validation of the simulation results has been carried out using a RBK robot, i.e., a real electric vehicle.

The work area is in the facilities of the Universitat Politècnica de València (UPV), Spain, and covers an area of 7200 m². It corresponds to the access area of the laboratory where the car-like robot is stored and extends over the ground floor of the university covering several buildings.

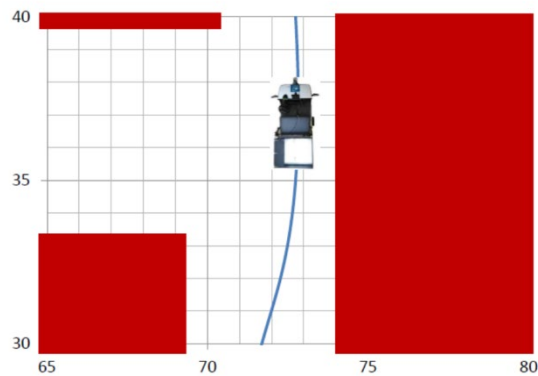
Finally, the example proposed in [27] will be solved and the results obtained will be compared. The vehicles used (in this paper and in [27]) are similar and have been characterized using the bicycle model.

5.1. First example.

The initial configuration is c_i (81.5m, 21.7m, 3.14 rad) and the target point p_f (70.0 m, 64.4 m). The solution required a computation time of $T_c = 281.25$ ms, obtaining a trajectory of $m=6$ intervals with a value of the objective function of $f(t)=33.91$ s.



a)



b)

Figure 6. a) Trajectory followed by the robot; b) Detail in the area approaching an obstacle (measured in meters).

Figure 6 shows the trajectory followed by the vehicle to avoid obstacles, as can be seen in the detail.

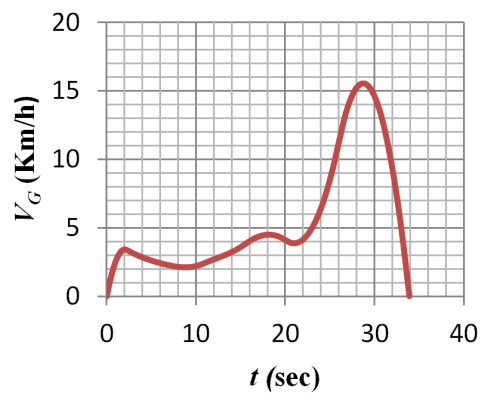


Figure 7. Evolution of the vehicle velocity throughout the trajectory.

Figure 7 shows the evolution of the vehicle velocity throughout the trajectory, where it is possible to observe how it increases with the radius of curvature. Whereas Figure 8 shows the evolution of the torque applied to the wheels to achieve the motion, where positive values are supplied by the engine through transmission and negative values by means of the brake system.

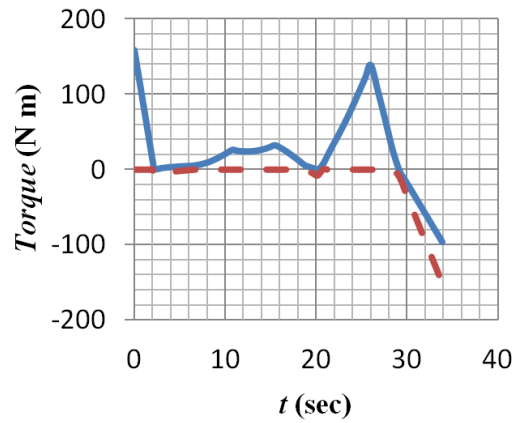


Figure 8. Evolution of the torque applied to the rear (solid line) and front (dashed line) wheels.
5.2. Second example.

The initial configuration is c_i (81.5 m, 21.7 m, 3.14 rad) and the target point p_f (63.5 m, 73.0 m). The solution required a computation time of $T_c=921.87$ ms, obtaining a trajectory of $m=6$ intervals with a value of the objective function of $f(t)=32.71$ s.

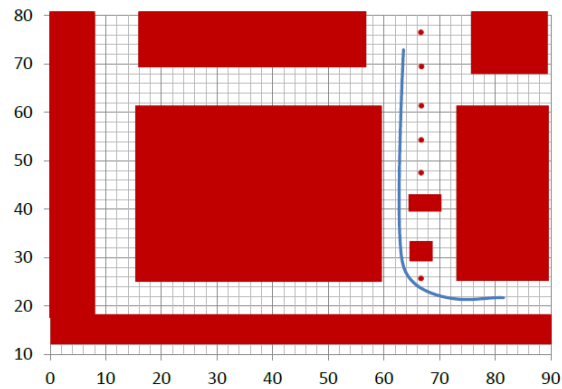


Figure 9. Trajectory followed by the robot in example 2 (measured in meters).

In Figure 9, it can be seen how the trajectory obtained has greater curvatures compared to Example 1. Thus, a higher speed is achieved and a lower time is taken (Figure 10), despite less torque being applied at the start (Figure 11), to reach a point close to the previous example.

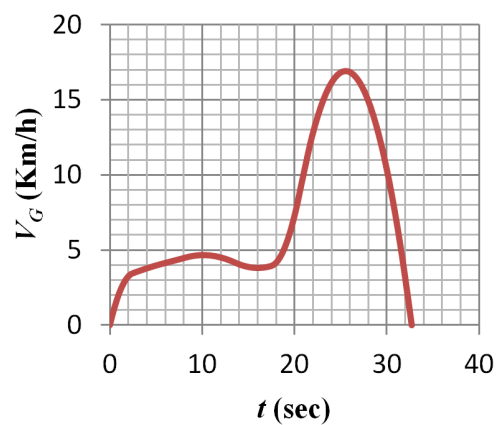


Figure 10. Evolution of the vehicle velocity throughout the trajectory.

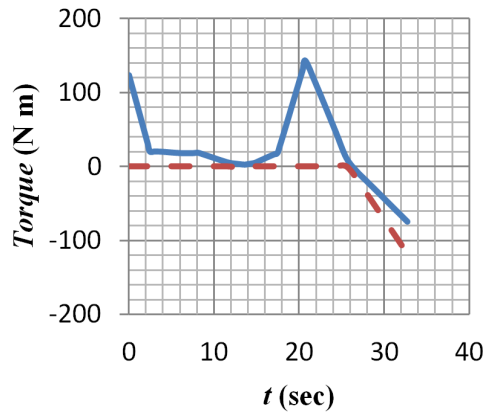


Figure 11. Evolution of the torque applied to the rear wheels (solid line) and front wheels (dashed line)

5.3. Third example.

The initial configuration is c_i (12.0 m, 75.0 m, 4.71 rad) and the target point p_f (81.5 m, 21.7 m). The solution required a computation time of $T_c=437.50$ ms, obtaining a trajectory of $m=6$ intervals with a value of the objective function of $f(t)=59.34$ s.

Figure 12 shows the trajectory traveled, its continuity and smoothness.

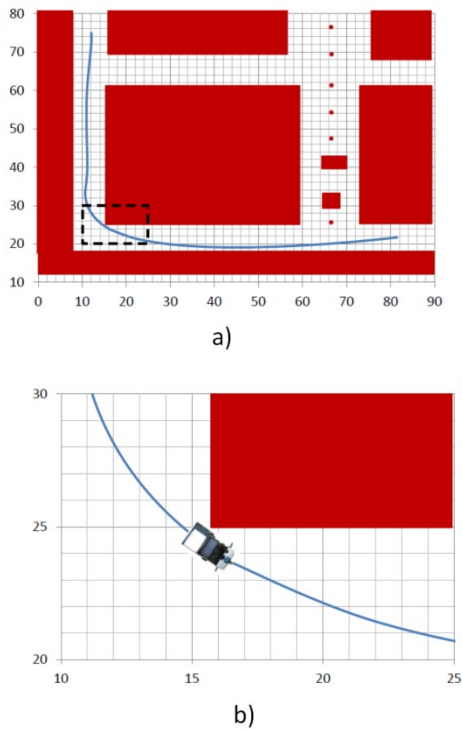
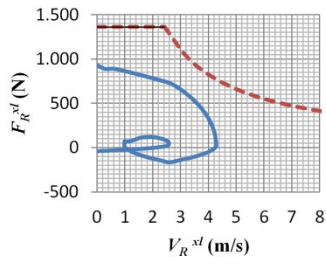
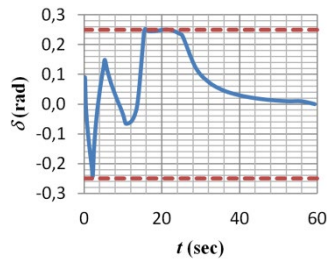


Figure 12. a) Trajectory followed by the robot; b) Detail in the area approaching an obstacle (measured in meters)

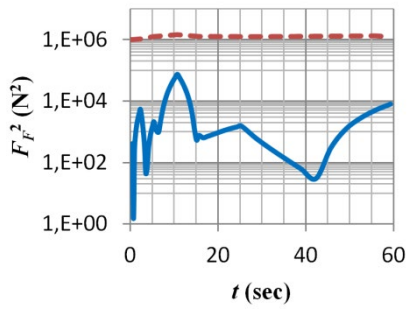


a)

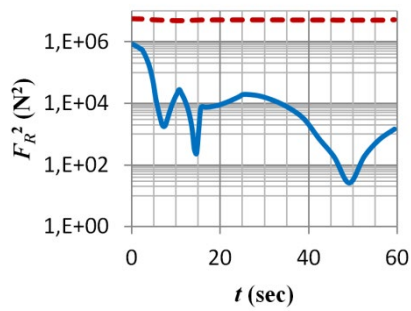


b)

Figure 13. (a) Longitudinal force on the rear wheel (solid line) and force limit available through the transmission (dashed line); b) Steering angle (solid line) and its limit (dashed line)
 Figure 13 shows the values associated with the limitations imposed by the torque and steering angle that are used in calculating the constraints using equations (31) and (18), respectively.

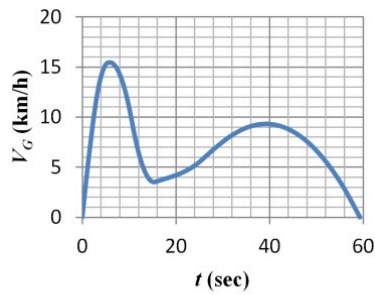


a)

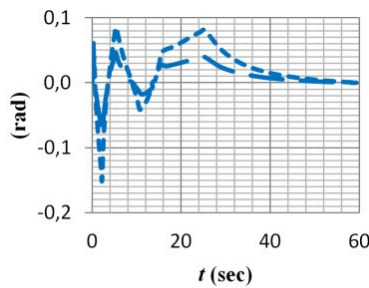


b)

Figure 14. Square of the resultant of the forces in the plane of the track mark (solid line) and square of the adhesion limit (dashed line): a) for the front wheel, b) for the rear wheel.



a)



b)

Figure 15. a) Velocity; b) Sideslip of the front wheels (long dashed line) and the rear wheels (short dashed line).

Figure 14 shows the values associated with the adhesion forces and their limits, which are used to calculate the constraints using equation (29).

Figure 15 a) shows the evolution of the velocity that is used in the constraint formulated in (19), and Figure 15 b) shows the evolution of the sideslip angles in the tires, which verify the validity of the hypotheses associated with them.

5.4. Fourth example.

In this example, in order to compare results, the dimensional and inertial characteristics of the RBK robot described in section 4.1 have been adapted to those of the 4WS4WD vehicle described in [27]. The main differences between the two vehicles mentioned are that 4WS4WD has four driving and steering wheels and it can consider a different coefficient of friction for each section in the path, while RBK has rear driving wheels, and steering on the front wheels and it uses the same coefficient of friction between the tires and the terrain for the entire trajectory (in this example 0.3). The trajectory, generated using the passing points described in [27] and without velocities constraints, can be seen in Figure 15.

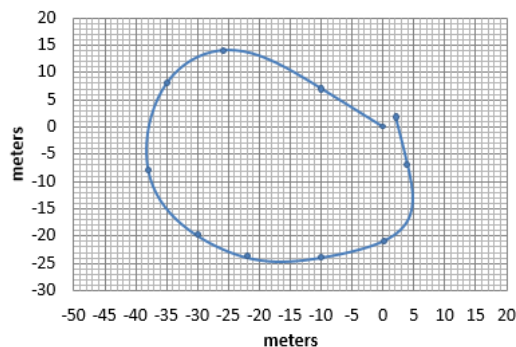


Figure 15. Trajectory followed by the vehicle.

Figure 15 shows the trajectory obtained under the conditions described above, where it can be seen how the resulting curvature is softer than the reference one.

The vehicle spends 36.5 seconds in performing the trajectory with the velocity profile shown in figure 16. Remember that there are no constraints imposed on the velocity at the passing points.

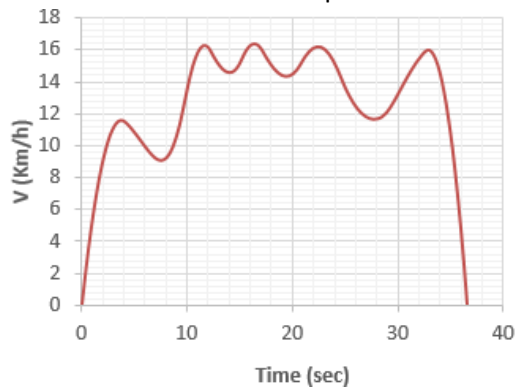


Figure 16. Longitudinal velocity

Figure 17 shows how the friction constraints are working in the front wheels along the trajectory, and it is possible to check how the limit is reached in different points.

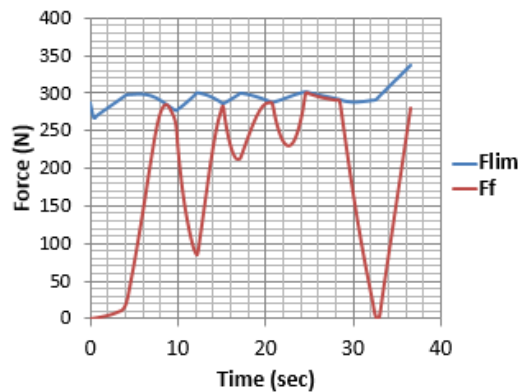


Figure 17. Friction limit, F_{lim} , and magnitude of the resultant longitudinal and lateral forces, F_f , on the front wheels

Figure 18 shows the evolution of the driving torque applied on the rear wheels. It can be seen how it takes negative values at some points given that it has braking capacity, and how the maximum values are consistent with those of the reference, considering that it is a vehicle with rear-wheel drive.

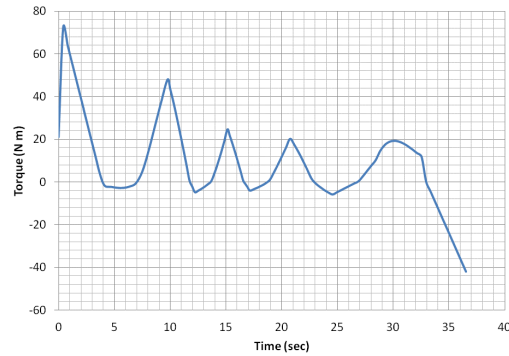


Figure 18. Driving torque applied on the rear wheels

6. CONCLUSIONS

A powerful optimization algorithm is developed for designing through AGVs efficient and flexible manufacturing and logistics systems within the facilities with the aim to increase the business performance.

The planner makes it possible to obtain safe and efficient trajectories in environments with stationary obstacles. Safety means not only the absence of collisions, but also the feasibility of the trajectory that is guaranteed based on compliance with the dynamic constraints of the mechanical system, which allows us to consider both the performance of the powertrain and the effects of the behavior of the tires or the load of the vehicle, among others parameters. On the other hand, the term efficiency is associated with the results, which do not guarantee the optimum trajectory, but they do make it possible to obtain trajectories that derive from an optimal one (conditioned by the interpolation functions that define the trajectory) and are adapted to the environment while being compatible with the dynamic limitations of the robot.

With respect to the example of reference [27], trajectories with softer radii of curvature are obtained.

Limitations as a global planner come from the models used to define the path and the dynamic behavior of the robot, since low-complexity algorithms are sought to reduce the computing times. These limitations have led to conservative results for the trajectories obtained.

Future work is associated with plans for a local planner that can be combined with the one presented in this article, which enables mobile obstacles to be detected by generating local variations of the trajectory to avoid collisions.

ACKNOWLEDGMENTS

This work was supported by the Spanish Ministry of Economy and Competitiveness, which has funded the DPI2013-44227-R project.

REFERENCES:

- [1] Brooks, R.A., 1983, Solving the find path problem by good representation of free space. IEEE Transactions on Systems, Man, and Cybernetics, 13(2): p. 190-197.

- [2] Eberhart, Y., Shi, 2001, Particle swarm optimization: developments, applications and resources, in *Evolutionary Computation. Proceedings of the 2001 Congress on Evolutionary Computation*.
- [3] Glavaski, D., Volf M., Bonkovic M., 2009, Mobile robot path planning using exact cell decomposition and potential field methods. *WSEAS Transactions on Circuits and Systems* 2009. 8(9).
- [4] Buniyamin N., Wan Ngah W.A.J., Sariff N., Mohamad Z., 2011, A Simple Local Path Planning Algorithm for Autonomous Mobile Robots. *International journal of systems applications, engineering & development*, 2- 5,
- [5] Yahja, A., Sanjiv Singh, Barry L. Brumitt. 1998, Framed-Quadtree Path Planning for Mobile Robots Operating in Sparse Environments, in *IEEE Conference on Robotics and Automation (ICRA)*. Leuven, Belgium
- [6] Singh, S., Simmons R., Smith T., Stentz A., Verma V., Yahja A., Schwehr K., 2000, Recent Progress in Local and Global Traversability for Planetary Rovers, in *IEEE Conference on Robotics and Automation*.
- [7] Sariff, N. and Buniyamin, N., 2006, An Overview of Autonomous Mobile Robot Path Planning Algorithms. 4th Student Conference on Research and Development. DOI: 10.1109/SCORED.2006.4339335
- [8] Rubio, F., Valero, F., Sunyer, J.L. and Mata, V., 2009, Direct step-by-step method for industrial robot path planning, *Industrial robot: an international journal*.36-6, pag.594-607.
- [9] Katrakazas, C., Quddus, M., Chen, W. H. and Deka, L., 2015, Real-time motion planning methods for autonomous on-road driving: State-of-the-art and future research directions. *Transportation Research Part C*, 60, 416–442
- [10] Pala, M., Eraghi, N. O., López-Colino, F.*, Sanchez, A., de Castro, A. and J. Garrido, 2013, HCTNav: A Path Planning Algorithm for Low-Cost Autonomous Robot Navigation in Indoor Environments. *ISPRS International Journal of Geo-Information*. 2, 729-748; doi: 10.3390/ijgi2030729
- [11] Gonzalez-Arjona, D.; Sanchez, A.; de Castro, A.; Garrido, J. Occupancy-Grid Indoor Mapping Using FPGA-Based Mobile Robots. In *Proceedings of the Conference on Design of Circuits and Integrated Systems*, Albufeira, Portugal, 16–18 November 2011; pp. 345–350.
- [12] Tokekar, P., Karnad, N. and Isler, V., 2014, Energy-optimal trajectory planning for car-like robots, *Autonomous Robots*. 37, pp. 279-300. DOI 10.1007/s10514-014-9390-3
- [13] Labakhua, L., Nunes, U., Rodrigues, R. and Leite, F., 2005, Trajectory planning methods for autonomous car-like vehicles. *The International Symposium on System Theory, Automation, Robotics, Computers, Informatics, Electronics and Instrumentation (ace.ucv.ro/sintes12/sintes12_2005/mechatronics/m7.pdf)*
- [14] Ghita, N. and Kloetzer, M., 2012, Trajectory planning for a car-like robot by environment abstraction. *Robotics and Autonomous Systems* 60 (2012) 609–619.
- [15] Li, X., Sun, Z., Cao, D., Liu, D. and He, H., 2017, Development of a new integrated local trajectory planning and tracking control framework for autonomous ground vehicles. *Mechanical Systems and Signal Processing*. 87, 118–137
- [16] Li, B. and Shao, Z., 2015, Simultaneous dynamic optimization: A trajectory planning method for nonholonomic car-like robots. *Advances in Engineering Software*, 87, 30–42

- [17] Wang, D. and Qi, F., 2001, Trajectory Planning for a Four-Wheel-Steering Vehicle. Proceedings of the 2001 IEEE International Conference on Robotics & Automation. (<http://www.ntu.edu.sg/home/edwwang/confpapers/wdwicar01.pdf>)
- [18] Schittkowski, K., 2010, NLPQLPA Fortran implementation of a sequential quadratic programming algorithm with distributed and non-monotone line search, Report, Department of Computer Science, University of Bayreuth.
- [19] Schittkowski, K., 2015, NLPQLP: A Fortran implementation of a sequential quadratic programming algorithm with distributed and non-monotone line search, User's Guide, Version 5.0.
- [20] Simba, K. R., Uchiyama, N., & Sano, S., 2014, Real-Time Obstacle-Avoidance Motion Planning for Autonomous Mobile Robots. Australian Control Conference
- [21] Simba, K. R., Uchiyama, N., & Sano, S., 2016, Real-time smooth trajectory generation for nonholonomic mobile robots using Bézier curves. *Robotics and Computer-Integrated Manufacturing*, 41, pp 31-42
- [22] Li, B., & Shao, Z., 2015. Simultaneous dynamic optimization: A trajectory planning method for nonholonomic car-like robots. *Advances in Engineering Software* 87, pp. 30–42
- [23] Tokekar, P., Karnad, N., & Isler, V., 2014, Energy-optimal trajectory planning for car-like robots. *Autonomous Robot*, 37, pp. 279–300
- [24] Chong, H. K. and Byung, K. K., 2007, Minimum-Energy Translational Trajectory Generation for Differential-Driven Wheeled Mobile Robots, *Journal of Intelligent and Robotic Systems*, 49, 4 pp 367-383. DOI 10.1007/s10846-007-9142-0
- [25] Rubio, F., Llopis-Albert, C., Valero, F. & Suñer, J.L., 2016, Industrial robot efficient trajectory generation without collision through the evolution of the optimal trajectory. *Robotics and Autonomous Systems*, 86, pp. 106–112
- [26] Suñer, J.L., Valero, F., Ródenas, J.J. & Besa, A. 2007 . Comparación entre procedimientos de solución de la interpolación por funciones splines para la planificación de trayectorias de robots industriales. ISBN: 978-9972-2885-31.
- [27] Dai, P., Taghia, J., Lam, S., Katupitiya, J., 2018, Integration of sliding mode based steering control and PSO based drive force control for a 4WS4WD vehicle, *Autonomous Robots*, 42, 3, pp 553-568.
- [X] Li, H., Savkina, A.V., 2018, An algorithm for safe navigation of mobile robots by a sensor network in dynamic cluttered industrial environments. *Robotics and Computer-Integrated Manufacturing* 54, 65-82. DOI: 10.1016/j.rcim.2018.05.008.
- [X] Li, S., Sun, D., Zhu, C., 2014, A dynamic priority based path planning for cooperation of multiple mobile robots in formation forming. *Robotics and Computer-Integrated Manufacturing* 30(6),589-596. DOI: 10.1016/j.rcim.2014.04.002.
- [X] Llopis-Albert, C., Rubio, F., Valero, F., 2018, Fuzzy set/qualitative comparative analysis applied to the design of a network flow of automated guided vehicles for improving business productivity. *Journal of Business Research*, accepted.